# CHAPTER 6

This chapter consists of results of miscellaneous experiments that are not included in Chapters 3-5. The aims discussed in this chapter were:

1) to determine the antimalarial activity of artemisone and its metabolites in plasma samples (*ex vivo* activity) after oral administration of artemisone and artemisone entrapped in the Pheroid® to Vervet monkeys.
2) to determine the effect of artemisone and the Pheroid® on the generation of ROS formation within the malaria parasite.

# CHAPTER 6
# MISCELLANEOUS RESULTS

## 1. Introduction

The first study described in this chapter is the *ex vivo* bioassay study. Antimalarial activity in plasma or serum at an unknown concentration of a drug can be related to the known concentrations of the drug required for parasite growth inhibition according to the modified *in vitro* drug bioassay described by Teja-Isavadharm *et al.* (2004). This *ex vivo* bioassay is an efficient method for the comparative measurement of both the efficacy and bioavailability of an orally administered drug (Kotecka & Rieckmann, 1993). The aim of this study was thus to determine the antimalarial activity of artemisone and its metabolites in plasma samples (*ex vivo* activity) after oral administration of artemisone and artemisone entrapped in the Pheroid® to Vervet monkeys.

Three metabolites (M1-M3) of artemisone possess antimalarial activities. Although the metabolites are not as active as the parent drug, relatively high concentrations of the metabolites are present in the plasma after exposure to oral artemisone (Nagelschmitz *et al*., 2008). During the monkey pharmacokinetic (PK) study, unexpectedly low levels of artemisone were found in the plasma (see Chapter 3). This study was designed to try to explain whether the low bioavailability of artemisone in this study may have resulted from first-pass metabolism and the production of active metabolites. In the monkey PK study (Chapter 3), only the metabolite M1 was measured, but higher concentrations of the metabolite M1 were present than the parent compound artemisone. Therefore, the metabolites at high concentrations would make an additional contribution to the overall parasiticidal effect of artemisone in the plasma.

The second study carried out was designed to establish whether the application of artemisone to malaria parasites generates reactive oxygen species (ROS). One proposed mechanism of action of artemisinins is that since the artemisinins are peroxides, they generate ROS within the malaria parasite (Krungkrai & Yuthavong, 1987; Levander,*et al*., 1989; Meshnick *et al*., 1989). Artemisinin treatment also results in ROS production in isolated mitochondria from yeast and malaria but not in mammalian mitochondria (Wang *et al.,* 2010). In addition, ROS scavengers such as DPPD (*N*,*N*'-diphenyl-1,4-phenylenediamine), edaravone, dithiothreitol and alpha-tocopherol antagonize the antimalarial effect of artemisinin (Wang *et al*., 2010; Krungkrai & Yuthavong, 1987).

Neurotoxicity of the artemisinins is observed against brain stem cells *in vitro* (Wesche *et al*., 1994; Fishwick *et al.,* 1995; Mclean & Ward, 1998; Schmuck *et al*., 2002). Schmuck *et al.*

(2002) proposed that the neurotoxic effect may be related to the production of radicals and, in parallel, inhibition of the respiratory chain. Artemisone, however, unlike the first generation artemisinins, is not neurotoxic (Haynes *et al.,* 2006) and, therefore, it would be interesting to analyze the effect of artemisone on ROS production within the malaria parasite.

Even though the Pheroid® formulation contains the ROS scavengers alpha-tocopherol, butylatedhydroxyanisole (BHA), butylatedhydroxytoluene (BHT) and the ethyl esters of long chain unsaturated fatty acid, it was reported to increase the antimalarial efficacy of artemisinins (Steyn, 2010; Jourdan, 2011). However, as outlined in Chapter 4, we have established unambiguously that the Pheroid® formulation does not enhance the efficacy of artemisone. This finding is in line with the results reported from the Swiss Tropical and Public Health Institute (STPHI; Jourdan, 2011). Irrespective of this, it is of interest to establish if the Pheroid® exerts any effect on ROS production within the malaria parasite.

This plan was to label drug-treated *P. falciparum* samples with both the fluorescent nucleic acid-binding dye SYTO 61 and fluorescent reactive oxygen species reporter 5-(and-6)-chloromethyl-2',7'-dichlorodihydrofluorescein diacetate acetyl ester to measure oxidative stress at the different developmental stages of the intraereythrocytic malaria parasite. SYTO 61 allows one to distinguish between uninfected and infected erythrocytes. The membrane-permeant 5-(and-6)-chloromethyl-2′,7′-dichlorodihydro-fluorescein diacetate (CM-$H_2$DCFDA) probe is used for screening for intracellular oxidative stress (LeBel *et al*, 1992). Once inside the cell, it is deacetylated by esterases to produce the nonfluorescent 5-(and-6)-chloromethyl-2′,7′-dichlorodihydrofluorescein. Upon oxidation by reactive oxygen species (ROS), in particular $H_2O_2$ in the presence of iron or hematin, the highly fluorescent 2′,7′-dichlorodihydrofluorescein (DCF) product is formed (LeBel *et al*, 1992; Cathcart, *et a*l., 1983). There were some inherent issues with this approach: the artemisinins themselves may oxidize the 5-(and-6)-chloromethyl-2′,7′-dichlorodihydrofluorescein to the 2′,7′-dichlorodihydrofluorescein (DCF); in addition endogenous $Fe^{3+}$ alone will also oxidize the dihydrofluorescein and artemisinins are very likely to interfere with the reduced conjugate of SYTO-61 dye. Nevertheless, an attempt was made to investigate the effect of artemisone and artemisone entrapped in Pheroid®.

## 2. Materials and Methods

### 2.1. Materials

As for the other studies described in this thesis, artemisone and its metabolite M1 were prepared by Ho-Ning Wong and Wing-Chi Chan in the Department of Chemistry at the Hong Kong University of Science and Technology, Clear Water Bay, Kowloon, Hong Kong.

Vitamin F ethyl ester was obtained from Chemimpo (South Africa) and Kolliphor® EL was obtained from BASF (South Africa). Butylatedhydroxyanisole (BHA), butylatedhydroxytoluene (BHT), polyethylene glycol (PEG 400) and dl-α-tocopherol were obtained from Chempure (South Africa). Purified water was obtained from SABAX (Johannesburg, South Africa). RPMI 1640, 4-(2-hydroxyethyl)-1-piperazine-ethanesulfonic acid (HEPES), hypoxanthine, gentamycin, D-(+)-glucose powder, sodium bicarbonate, sodium chloride, sorbitol, hydrogen peroxide ($H_2O_2$), dimethyl sulfoxide (DMSO) were all obtained from Sigma Aldrich® (St. Louis, MO, USA). Albumax II was obtained from the Scientific Group, South Africa and from the Departmentt of Pharmacology, University of Cape Town. A three component gas mixture comprising 5% oxygen, 5% carbon dioxide and 90% nitrogen was obtained from Afrox (Germiston, South Africa). Giemsa stain, sodium phosphate and potassium phosphate were supplied by MERCK (South Africa). Affigel protein A (binding capacity of 20 mg of purified human immunoglobulin G [IgG]/mg of gel) was obtained from Bio-Rad (Richmond, California, USA.) SYTO 61 and 5-(and-6)-chloromethyl-2′,7′- dichlorodihydro-fluorescein diacetate acetyl ester (CM-$H_2$DCFDA) were obtained from Life Technologies Inc. (Paisley, UK). All other chemicals and reagents used in this study were of analytical reagent grade.

## 2.2. Methods

### 2.2.1. Preparation of drug solutions and plasma samples

For the drug susceptibility study, artemisone stock solutions (500 µM) were prepared in 100% acetonitrile and chloroquine (CQ) stock solutions (20 mM) were prepared in sterile water. Artemisone stock solutions (30 mM) were prepared in 100% acetonitrile, while artemether (30mM), artesunate (30 mM) and DHA (30mM) were prepared in ethanol. Subsequent dilutions were made in plain culture medium to obtain the desired experimental drug concentration. SYTO 61 (100 µM) were prepared in DMSO; CM-DCFDA (1 mM) and $H_2O_2$ (100 mM) were freshly prepared before each experiment in ethanol and water respectively. Subsequent dilutions were made in PBS or medium to obtain the desired experimental drug concentration.

For both the *ex vivo* bioassay and ROS assays, drug-free pro-Pheroid® with manufacturing batch number P12006 was used for all dilutions while artemisone (500 µM) containing pro-Pheroid® (P12012) was used in the drug susceptibility assays and artemisone (30 mM) containing pro-Pheroid® (P12010) was used in the ROS assays. The pro-Pheroid® formulations used in these studies were prepared according to the ratios summarized in Table 1. Briefly, the Pheroid® formulations were prepared by dissolving artemisone in PEG

400, heating to 70˚C and sonicating. Vitamin F ethyl ester, Kolliphor® EL, BHA and BHT were added to the mixture that was heated to 70˚C and sonicated. d,l-α-tocopherol was then added and the mixture gassed with nitrous oxide ($N_2O$) under pressure (200 kPA) for four days. To prepare saturated nitrous oxide water, sterile water for injection was gassed with nitrous oxide ($N_2O$) under pressure (200 kPA) for four days. The saturated nitrous oxide water was used to dilute the Pheroid® stock solutions before diluting with plain culture medium to obtain the correct artemisone concentration and Pheroid® dilution.

**Table 1:** The composition of the Pheroid® formulations used in the drug susceptibility and ROS studies.

| Component/ Pheroid batch | P12006 (drug free) (g) | P12012 (0.5 mM artemisone) (g) | P12010 (30 mM artemisone) (g) |
|---|---|---|---|
| Vitamin F ethyl ester | 66.49 | 66.41 | 65.57 |
| Kollifor® EL | 27.67 | 27.66 | 27.32 |
| dl-α- tocopherol | 1.00 | 1.00 | 1.00 |
| PEG 400 | 4.90 | 4.90 | 4.90 |
| BHA | 0.01 | 0.01 | 0.01 |
| BHT | 0.01 | 0.01 | 0.01 |
| Artemisone | - | 0.02 | 1.2 |

To characterize the Pro-Pheroid® formulations, these were mixed with 0.1 N hydrochloric acid (1:100 v/v) and the size and surface charge (zeta potential) of the resulting Pheroid® vesicles were measured with a HydroMalvern Mastersizer 2000MU and a Malvern 2000 zetasizer (Malvern Instruments Ltd, Malvern, Worcestershire, UK). For particle size measurement, samples were measured in duplicate by diluting samples with water before injectionandfor surface charge measurements samples were measured in triplicate. The morphology of the particles was characterized by confocal laser scanning microscopy (CLSM, Nikon D-eclipse C1 confocal laser scanning microscope) by staining the Pheroid® formulations with Nile Red. Briefly, Pheroid® vesicles were stained with Nile Red (50:1 v/v) at room temperature for 15 minutes in the dark and analysed, using a He/Ne laser. Samples were placed on microscope slides, covered with a glass coverslip and analysed.

Plasma samples collected from healthy monkey subjects during the PK study (Chapter 3) were collected prior to (T0) and at 0.5, 1, 2, 3, 5, 8 and 10 hours post treatment and stored at -80℃. For the bioassay treatment of erythrocytes, the T0 plasma samples remarkably caused a dramatic decrease in the number of *P. falciparum*-infected erythrocytes *in vitro*

(Figure 4 below). This may be caused by the lysis of *P. falciparum*-infected erythrocytes via complement-mediated lysis of cells bound with immunoglobulin (Gabriel & Berzins, 1982). Therefore, in an effort to inhibit complement-mediated lysis, plasma samples were treated with Affigel protein A or heat inactivated according to the methods described by Teja-Isavadharm *et al*. (2004). Briefly, 50 µl of Affigel protein A was washed twice with 50 µl of phosphate-buffered saline (PBS, pH 7.4) and then with 50 µl of RPMI 1640 medium by centrifugation for 5 seconds. Then, the supernatant was discarded and 250 µl plasma was incubated with the protein A gel for 30 min at room temperature. For heat inactivation, the plasma samples were heated at 56℃ for 30 min. To obtain monkey plasma with known artemisone concentrations, drug-free monkey plasma was spiked with the same artemisone stock solution used in the drug susceptibility assay.

### 2.2.2. *In vitro cultivation of P. falciparum*

The *P. falciparum* 3D7 strain was maintained by the *in vitro* culture technique of Trager and Jensen (1976). Malaria parasites were cultured with a general parasitaemia of <5% and a 5% haematocrit (v/v) red blood cell suspension, in RPMI culture medium supplemented with glucose (4 g/L), hypoxanthine (0.04 g/L), HEPES (6g/L), sodium bicarbonate (0.2% solution), 0.5% Albumax II and gentamicin (0.048 g/L). The culture medium was changed once a day to maintain physiological pH (~7.4) and incubated at 37ºC in an atmosphere of 5% $CO_2$,5% $O_2$ and 90% $N_2$. During routine cultivation and before each experiment, thin blood smears were prepared, stained with giemsa stain and observed microscopically. The parasitaemia was determined by the total number of parasites and their various developmental stages per 1,000 RBC and parasitaemia was expressed as the number of infected red blood cells (IRBC) per 100 RBCs. Cultures were routinely synchronized every 48 hours when they were in the early ring stage by treating them with 5% D-Sorbitol (Lambros and Vanderberg; 1979). Briefly, five pellet volumes of 5% D-sorbitol was added to the cultures, mixed well and incubated at 37 ºC for 10 minutes. Thereafter it was centrifuged for 5 minutes at 2000 rpm and washed thrice with culture medium before adding fresh medium to the cultures.

### 2.2.3. *In vitro* and *ex vivo* antimalarial activities of artemisone against *P. falciparum*

All assays were carried out in sterile 96 well, flat-bottomed microculture plates. Drugs were serially diluted on separate plates. The artemisone reference formulation was diluted by using serum free culture medium, while the artemisone entrapped in Pheroid® was diluted with a constant Pheroid® dilution in serum free culture medium (either 0.001 or 0.002% oil phase Pheroid® dilution) in order to obtain a constant Pheroid® concentration throughout the dilution. Monkey plasma containing drug was diluted with drug-free plasma in the wells of a

microplate. Culture medium (40 µl) and 10 µl of the appropriate antimalarial drug(s) or plasma samples in wells of plates were inoculated with 50 µl of the parasitised RBCs (95 – 100% rings, 1% parasitaemia, 1% haematocrit) suspension. After inoculation, the plate covers were replaced and the plates were placed in an airtight incubation chamber and shaken gently. The chamber was flushed for 4 minutes with 5% $O_2$, 5% $CO_2$ and 90% $N_2$ and incubated at 37℃ for 48 hours. The chamber was re-gassed every 24 hours.

Antimalarial activity was assessed by the inhibitory effect of the drugs on the growth and development of malaria parasites. Drug-free medium was used as negative control and chloroquine (0.5 µM) as positive control. Antimalarial activity was assessed using the SYBR green assay (Smilkstein *et al.,* 2004, Bennet *et al.,* 2004). Briefly, after incubation, 100µl of the incubated samples were added to 100 µl freshly prepared SYBR green lysis buffer. SYBR green buffer was prepared by adding SYBR green II (0.2 µl/ml; Molecular Probes Inc) in lysis buffer (20 mM Tris, pH 7.5; 5 mM EDTA, 0.008% (w/v) saponin, 0.08% (v/v) triton X-100). Samples were measured after an 1 hour incubation at room temperature at excitation 485 nm, emission 530 nm using a Fluoroskan Ascent FL microplate fluorometer (Thermo Scientific). The data, after subtraction of background (CQ treated positive control, no parasite growth) were expressed as percentage of untreated control to determine cell proliferation and averaged from at least 3 independent experiments (±SD), unless otherwise stated.

For the *in vitro* drug susceptibility study three independent experiments were performed, each in triplicate. The $IC_{50}$ values were determined by estimating the drug concentrations that inhibited parasite growth by 50% relative to drug-free control cultures by fitting to a sigmoid dose response curve generated with PRISM software (Graphpad Software Inc.). Growth inhibition activity of Vervet monkey plasma *ex vivo* was compared to a standard curve generated for artemisone as a reference control (*in vitro* drug susceptibility data and spiked monkey plasma). Thereafter the *in vitro* and *ex vivo* pharmacodynamic area under the concentration-time curve from zero to 10 h ($AUC_{0-10}$) and maximum drug concentration ($C_{max}$) measurements were compared with corresponding pharmacokinetic measurements.

### 2.2.4. Determination of oxidative stress formation by artemisone reference and pro-Pheroid® formulation

Synchronized infected RBCs were harvested at the trophozoite stage, washed twice with serum free culture medium by centrifugation at 2000 rpm for 1 minute and resuspended (at 2% hematocrit) in serum-free medium containing 1–10 µM CM-H2DCFDA for 30 min, in the dark at 37˚C, before washing twice in PBS, pH 7.4 by centrifugation at 2000 rpm for 1

minute. Samples were then treated with serum-free medium containing the respective drugs for 2 hours at 37˚C, before washing twice in PBS, pH 7.4. Samples were then treated with serum-free medium containing 0.5 µM SYTO 61 for 45 min at room temperature. After this, samples were diluted with PBS or medium, maintained at 20˚C and analyzed as quickly as possible.

Flow cytometric measurements were performed on a FACSCalibur™ cytometer (Becton Dickinson). The channels and probes were green (DCF and fluorescein-dextran; 488 nm excitation, emission 530/30 nm) and red (SYTO 61; 633 nm, 660/20 nm). Samples were diluted with PBS or medium and 100,000 – 200,000 events (encompassing uninfected and infected RBCs) were acquired. The parasitized erythrocyte populations were selected by gating, as reflected on two dimensional scattergrams (see also Region 2, Figure 7 of results). Detector gain settings were varied between experiments to optimize signals but were kept constant within individual experiments. No compensation was applied to any of the channels. Values reported correspond to the average median signal intensity (MSI) of a particular population as measured in duplicate or triplicate

### 2.2.5. Statistical analysis

Statistical analysis was performed at a significance level of $p<0.05$ with a two tailed paired t-test using the PRISM software (Graphpad Software Inc.). $IC_{50}$ values were determined by fitting data to a sigmoid dose response curve generated with PRISM software (Graphpad Software Inc.).

## 3. Results

### 3.1. Pro-Pheroid® characterization

The particle size and zeta potential distribution of the Pheroid® formulations are summarized in Table 2. The span value, as an index of polydispersity, of the formulations was calculated by means of the equation $(d_{0.9} – d_{0.1})/ d_{0.5}$ where $d_{0.9}$, $d_{0.5}$ and $d_{0.1}$ are the particle diameters determined respectively at the $90^{th}$, $50^{th}$ and $10^{th}$ percentile of the particles.

**Table 2:** The particle size of the different Pheroid® formulations

| Pheroid® formulations | Mean particle size (µm) | $d_{0.1}$ (µm) | $d_{0.5}$ (µm) | $d_{0.9}$ (µm) | Span | Zeta potential (mV) |
|---|---|---|---|---|---|---|
| P12006 | 12.38 ± 0.97 | 3.09 ± 0.04 | 8.48 ± 0.53 | 26.41 ± 2.68 | 2.74 ± 0.15 | -0.64 ± 0.79 |
| P12012 | 2.3 ± 0.00 | 0.74 ± 0.00 | 1.74 ± 0.00 | 4.24 ± 0.01 | 2.01 ± 0.00 | 1.15 ± 1.48 |
| P12010 | 12.63 ± 0.25 | 3.30 ± 0.17 | 10.73 ± 0.34 | 24.10 ± 0.28 | 0.69 ± 0.00 | nd |

All formulations had a relatively low zeta potential due to the formulations containing PEG. Although PEG decreases the zeta potential, aggregation is inhibited since the steric distance between the particles are increased and the amount of attraction between nanoparticles decreased (Jokerst *et al*., 2011). The confocal laser scanning microscopy images of the Pheroid® formulations indicate the formation of spherical particles (Figure 2).

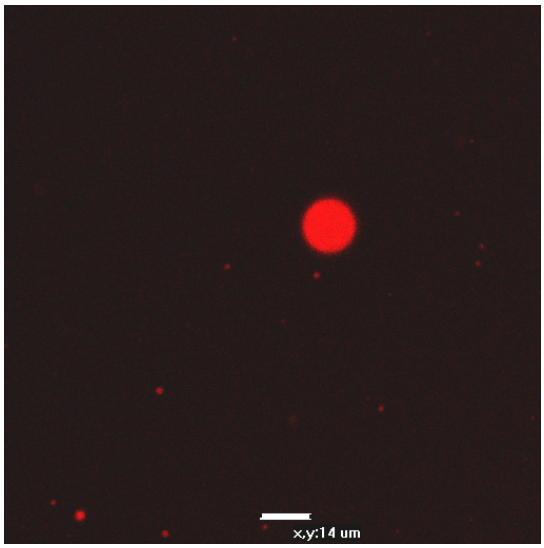


**Figure 1:** Confocal laser scanning electron microscopy micrograph of the Nile Red stained Pheroid® formulation (P12006).

### 3.2. *In vitro* and *ex vivo* antimalarial activities of artemisone against *P. falciparum*

When artemisone was entrapped in the Pheroid® drug delivery system, it showed statistically enhanced antimalarial activity ($p<0.05$) when compared to the artemisone reference against the *P. falciparum* 3D7 strain. The artemisone reference formulation had an $IC_{50}$ of 3.35 ± 0.82 nM, while the artemisone test formulation had $IC_{50}$ values of 1.07 ± 0.29 and 1.55 ±

0.58 nM for the 0.001 % and the 0.002 % pro-Pheroid® concentrations respectively (Figure 2). The $IC_{50}$ values of the two artemisone test formulations were not statistically different.

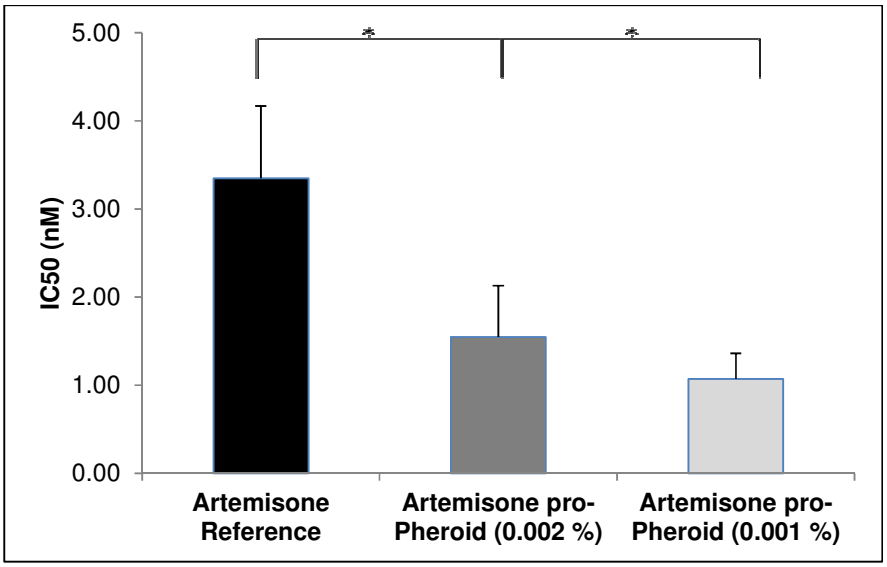


**Figure 2:** Effect of the Pheroid® formulation on the antimalarial activity of artemisone. Values represent the mean $IC_{50}$ ± SD (nM) from independent experiments (n≥3) performed in triplicate. * p< 0.05

Plasma from one monkey decreased parasite proliferation to <15% (Figure 3). This may be caused by the lysis of *P. falciparum*-infected erythrocytes via complement-mediated lysis of cells bound with immunoglobulin (Gabriel & Berzins, 1982).

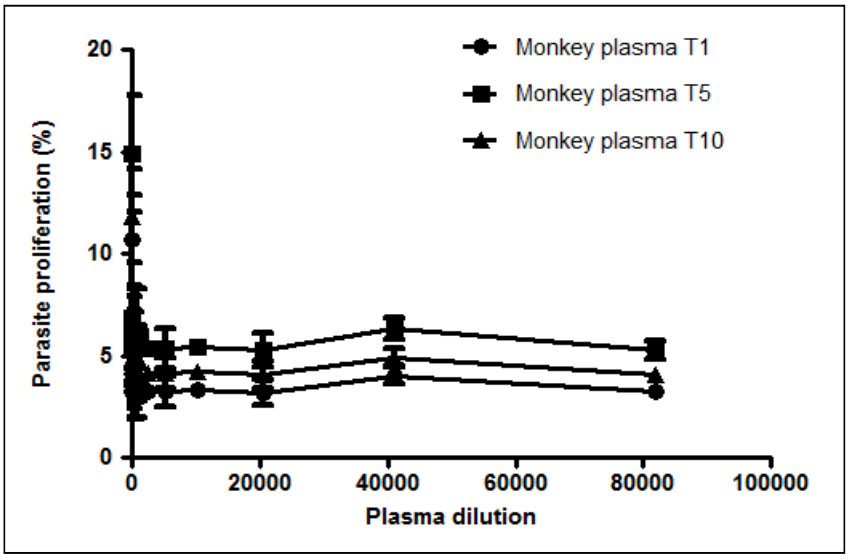


**Figure 3:** The effect of plasma dilutions from plasma collected from three time intervalson parasite proliferation. Values are depicted as mean ± SD

Drug free plasma was diluted with culture medium to determine the minimum dilution of the plasma that did not have an effect on the parasite proliferation. As indicated, 100% parasite growth was only obtained once the plasma was diluted approximately 500 fold. This meant that all plasma samples either had to be diluted 500 fold before antimalarial activity could be calculated (Figure 4). Due to the low artemisone concentration in the plasma, this was not possible. Therefore, the complement-mediated lysis of *P. falciparum* infected cells had to be inactivated either by heat inactivation or by treatment with Affigel protein A.

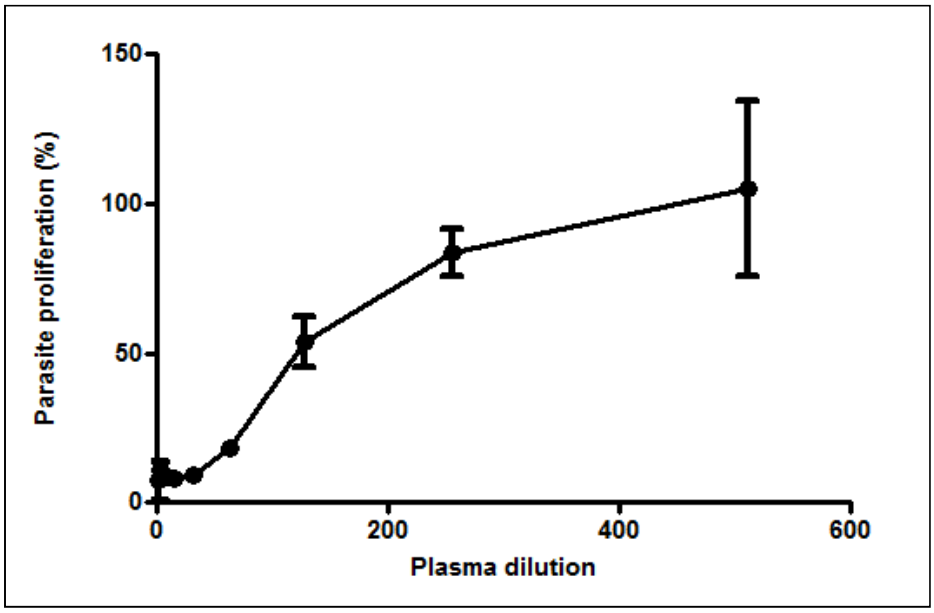


**Figure 4:** The effect of drug free plasma concentration on the parasite proliferation. Values are depicted as mean ± SD

Drug free plasma was then spiked with artemisone stock solution to a concentration of 500 nM artemisone. To reduce the growth-inhibitory activity of normal plasma, the spiked plasma sample and drug free plasma samples were heat inactivated. The heat inactivated plasma sample was used to make serial dilutions of the spiked plasma samples and parasite proliferation measured. As illustrated in Figure 5, the $IC_{50}$ of the artemisone spiked plasma could not be calculated since the parasite growth was still 83.50 ± 10.70% at the highest artemisone concentration used (5 nM), when compared to the drug free control. Therefore, either the concentration of artemisone had to be increased or Protein A inactivation of the plasma had to be considered, since heat inactivation of the artemisone spiked plasma samples might have decreased the activity of artemisone.

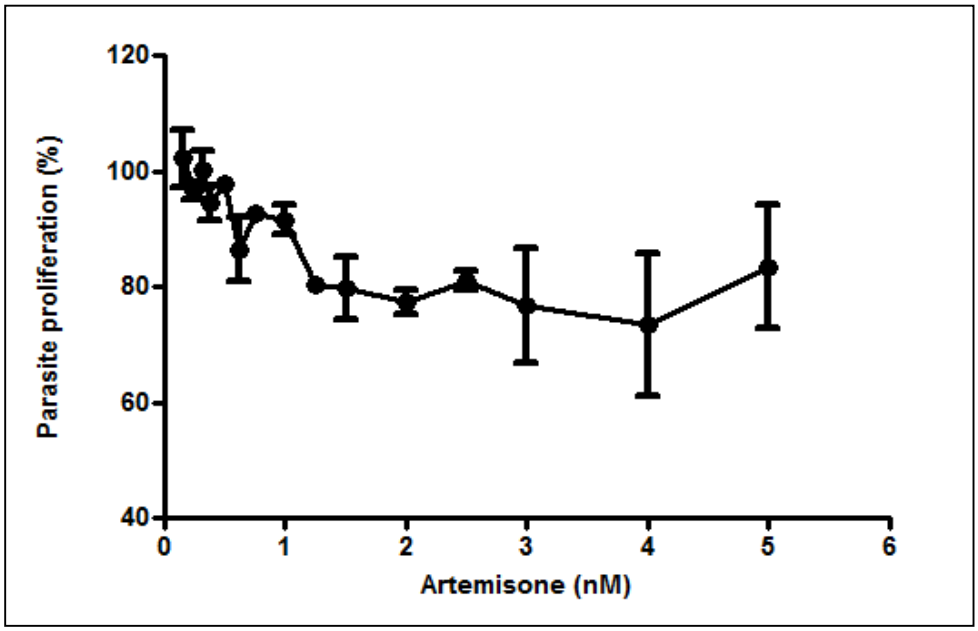


**Figure 5:** The effect of heat inactivated artemisone spiked plasma concentration on parasite proliferation. Values are depicted as mean ± SD.

Drug free plasma was spiked with artemisone stock solution to a concentration of 500nM artemisone and treated with either heat inactivated or Protein A. The highest concentration of artemisone spiked samples was increased from 5 to 50 nM. The resulting $IC_{50}$ values of 3.05 nM for heat inactivated plasma samples compared well with the *in vitro* artemisone $IC_{50}$ values (3.35 ± 0.82 nM) while the Protein A treated samples had a slightly lower $IC_{50}$ value of 1.32 nM (Figure 6).

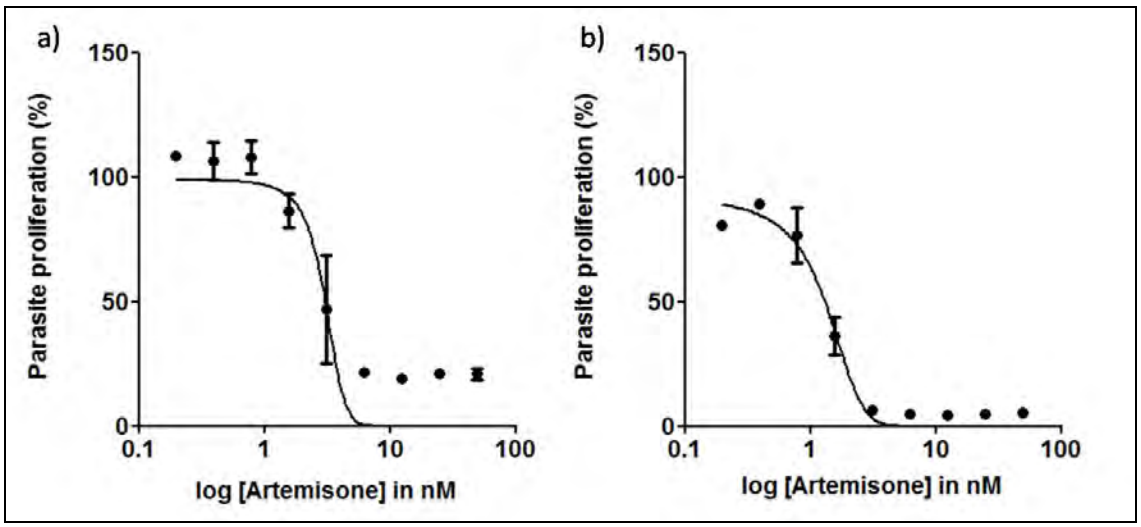


**Figure 6:** The effect of (a) heat inactivated and (b) protein A inactivated artemisone spiked plasma concentration on the parasite proliferation. Values are depicted as mean ± SD.

In an effort to repeat these results, experiments were repeated three times by spiking fresh drug-free plasma each time and inactivating the plasma by both methods. The results could not be reproduced, with no growth inhibition obtained during 5 subsequent independent experiments where different plasma samples were combined, spiked and treated. Therefore, artemisone samples from different time intervals from the PK study could not be used in the bioassay since the assay could not be validated. Plasma samples collected from healthy monkeys during the PK study (Chapter 3) could not be used in the bioassay since the method was not reproducible and was not sensitive enough for the detection of the anti-malarial activities of artemisone in monkey plasma.

### 3.3. Determination of ROS formation in *P.falciparum* parasites

The intraerythrocytic malaria parasite develops through ring (0 to 20 h), trophozoite (20 to 36 h), and schizont (36 to 48 h) stages. The rate of metabolism of the parasite increases as it enters the trophozoite stage since protein, lipid and nucleotide synthesis are required for rapid parasite growth. During this stage, the parasites consume host haemoglobin. This haemoglobin is degraded in the parasite food vacuole and subsequently superoxide ($O_2$•–) is produced that is rapidly converted into hydrogen peroxide ($H_2O_2$) either via superoxide dismutase or via direct reduction (Becker *et al.*, 2004).

Aliquots of uninfected and tightly synchronized infected RBCs were labelled with SYTO 61 and CM-$H_2$DCFDA at 5-15 h post-invasion (early rings) and 24–34 h (trophozoites). Results are illustrated by means of two-dimensional plots (Figure 7) of the fluorescence intensities in uninfected and infected red blood cells of different stages labelled with SYTO 61 and CM-$H_2$DCFDA. With the uninfected red blood cells, for SYTO 61, the average median signal intensity (MSI) in the uninfected red blood cell gate (Region 1; R1) is 12.52 ± 5.14 with only a only a small percentage of the population observed in the infected red blood cell gate (Region 2; R2). With the early rings and the trophozoites, the parasites form clear populations with MSI values of 530.48 ± 37.56 and 2132.38 ± 52.45 respectively. This indicates that SYTO 61 was successful in distinguishing the different stages of the infected parasites. The ring stage parasites exhibit a DCF signal that is slightly higher (MSI of 6.98 ± 0.78) than that of the uninfected RBCs (MSI of 5.90 ± 0.16) and the trophozoite stage parasites (MSI of 5.06 ± 0.14) are associated with a ~2 fold higher DCF signal (MSI 14.94 ± 3.81). Fu *et al.* (2010) observed ~5 fold higher MSI signal intensities in the trophozoite stage parasites when compared to the uninfected and ring stage parasites.

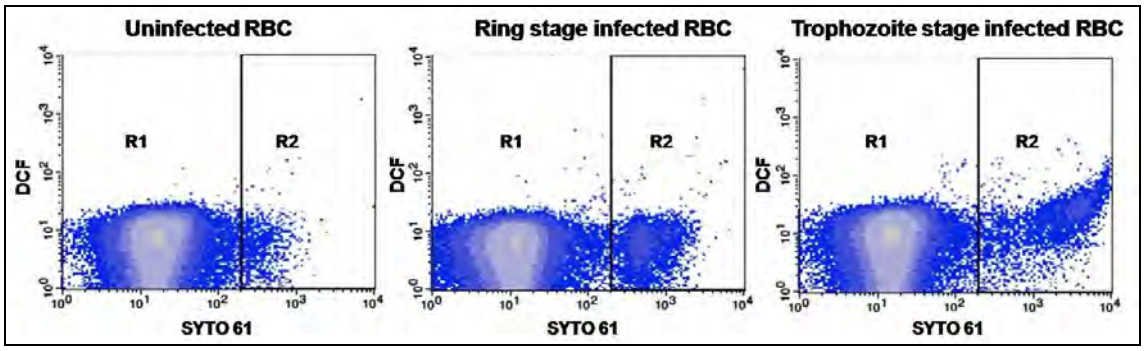


**Figure 7:** Two-dimensional plots of the DCF fluorescence and SYTO 61 fluorescence in uninfected, ring and trophozoite stage infected red blood cells analyzed by flow cytometry.

Trophozoite infected red blood cells were treated with $H_2O_2$, CQ and artemisone (concentration range 3.4-200 nM) for 2 h. The DCF signals from each drug treatment did not differ significantly from the DCF signals observed for the drug free control (Figure 8), indicating no increased oxidative insult in the parasite cytoplasm. This indicates that artemisone did not induce ROS production in the malaria parasite, even at the highest concentration of 200 nM. Since CM-$H_2$DCFDA is a probe designed to measure $H_2O_2$ and other ROS in cells, one would expect the DCF signals to be elevated with the $H_2O_2$ treated samples, which is not the case in this experiment.

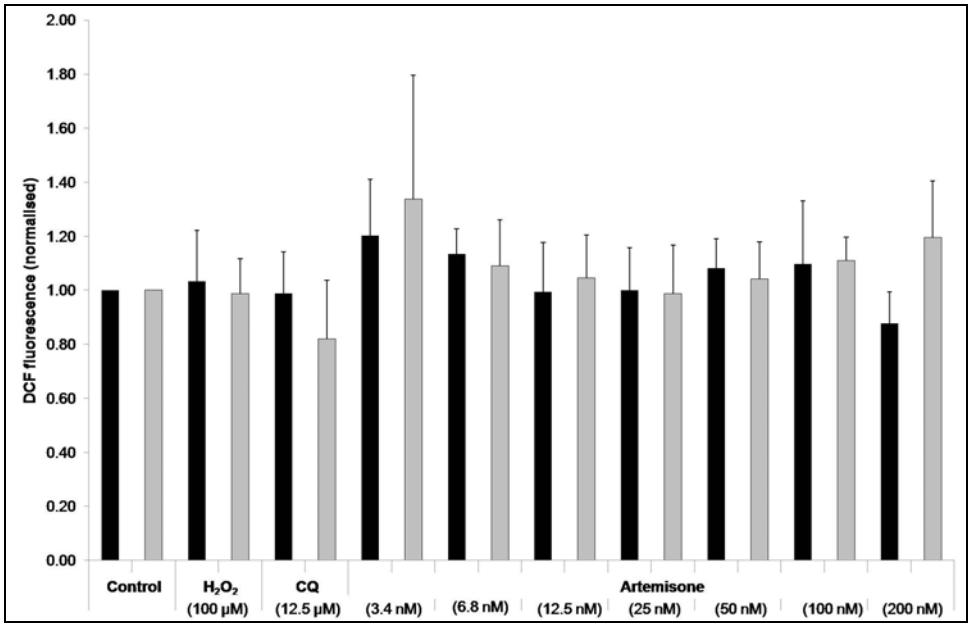


**Figure 8:** DCF fluorescent signals obtained with drug treatment of trophozoite stage parasites. Black bars depict samples where no pro-Pheroid® was added while the grey bars depict added pro-Pheroid® to the samples. Data are normalized to untreated controls. Values are depicted as mean ± SD from one experiment done in triplicate.

Because the DCF signal did not increase upon application of artemisone, the possibility exists that artemisone does not increase ROS production in the malaria parasite. Therefore, to confirm this, the reference drug DHA was used in the following experiment. DHA and artemisinin are reported to increase the DCF signal of trophozoite stage parasites labelled with SYTO 61 and CM-$H_2$DCFDA (Klonis *et al.*, 2011).

Two identical independent experiments were performed and combined results of these experiments are depicted in Figure 10. Results from these two experiments do not compare well. Results with $H_2O_2$ were not repeatable. With the one experiment $H_2O_2$ increased the DCF signal while the other experiment did not indicate an increase. Both artemisone and DHA did not increase the DCF signal.

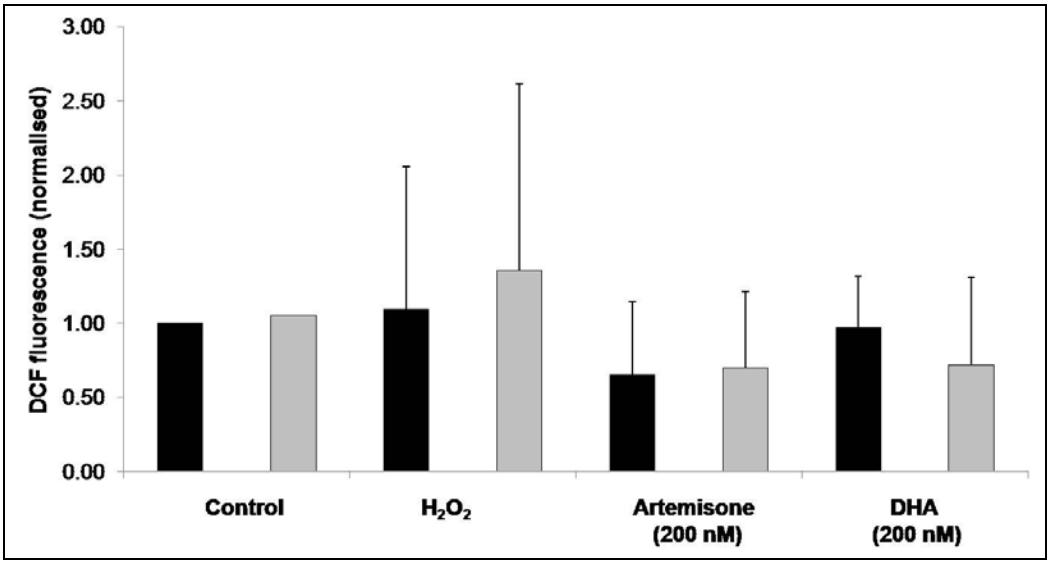


**Figure 9:** DCF fluorescent signals obtained with drug treatment of trophozoite stage parasites. Black bars depict samples where no pro-Pheroid® was added while the grey bars depict added pro-Pheroid® to the samples. Data are normalized relative to untreated controls. Values depicted as mean ± SD from two independent experiments performed in triplicate.

Since neither DHA nor the artemisinins increased the DCF signal, it was decided to incorporate other artemisinins in the study. Other parameters that were changed included the concentration and incubation time of labelling with the CM-$H_2$DCFDA probe and replacing PBS with medium. The concentration of CM-$H_2$DCFDA was increased from 1µM to 5 µM to ensure that the concentration of the probe is not the reason for the lack of DCF signal increase with drug treatment. The time of incubation with CM-$H_2$DCFDA was changed from 30 minutes to 15 minutes. RPMI supplemented with glucose (4 g/L),

hypoxanthine (0.04 g/L), HEPES (6 g/L), sodium bicarbonate (0.2% solution) and gentamicin (0.048 g/L) was used instead of PBS for all drug dilutions and parasite suspensions.

Infected red blood cells were treated with $H_2O_2$, DHA, artemisinin and artemisone. The DCF signals from each drug treatment (except for $H_2O_2$) did not differ significantly from the DCF signals observed for the drug free control (Figure 10). For the first time the positive control, $H_2O_2$, resulted in significantly higher ($p<0.05$) DCF signals when compared to the drug free controls in both of the two independent experiments.

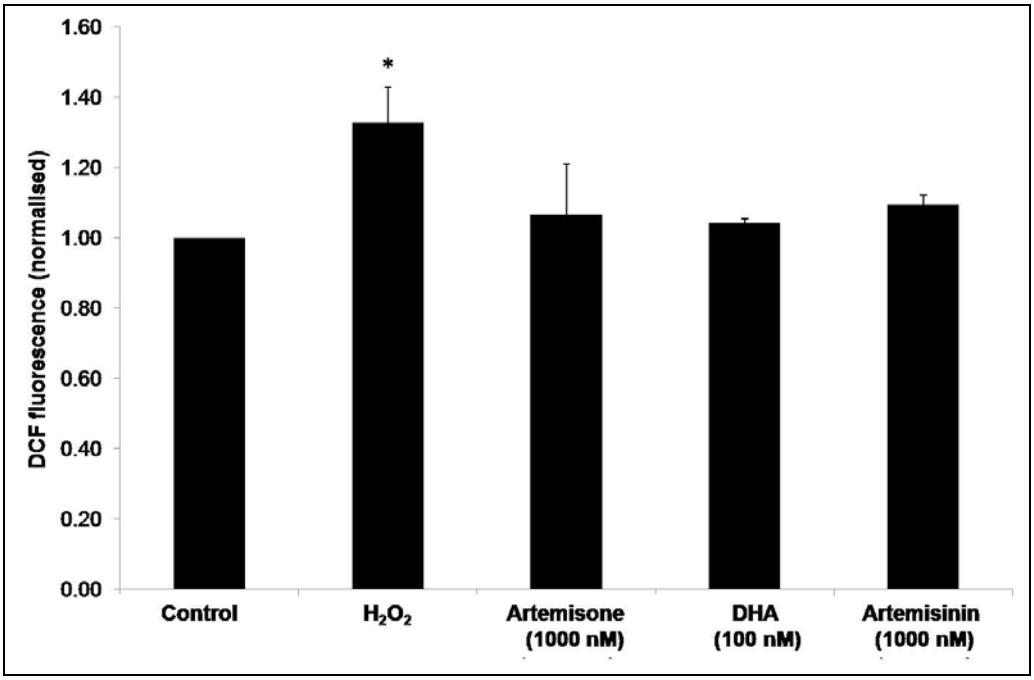


**Figure 10:** DCF fluorescent signals obtained with drug treatment of trophozoite stage parasites. Data are normalized to untreated controls. Values are depicted as mean ± SD from two independent experiments done in triplicate.*$p<0.05$.

Furthermore, infected red blood cells were treated with $H_2O_2$, DHA, artemisinin, artemether, artesunate and artemisone. The DCF signals from each drug treatment did not differ significantly from the DCF signals observed for the drug free control (Figure 11). Again, the positive control, $H_2O_2$, did not increase the DCF signals.

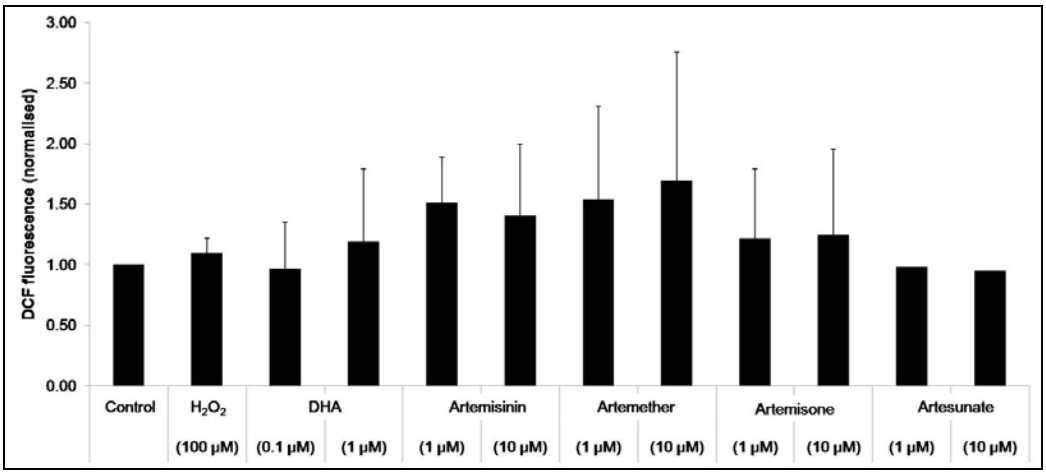


**Figure 11:** DCF fluorescent signals obtained with drug treatment of trophozoite stage parasites. Data are normalized to untreated controls. Values are depicted as mean ± SD from three independent (except for artesunate, which was from one experiment) experiments done in triplicate.

The study was repeated in unsupplemented RPMI medium (pH adjusted to 7.4) instead of RPMI medium supplemented with glucose (4 g/L), hypoxanthine (0.04 g/L), HEPES (6 g/L), sodium bicarbonate (0.2% solution) and gentamicin (0.04 g/L). This was done to evaluate if the additives had an effect on DCF fluorescence. The drug treated parasites did not differ significantly with the drug free control (Figure 12) and, therefore, the additives did not have an effect on the assay.

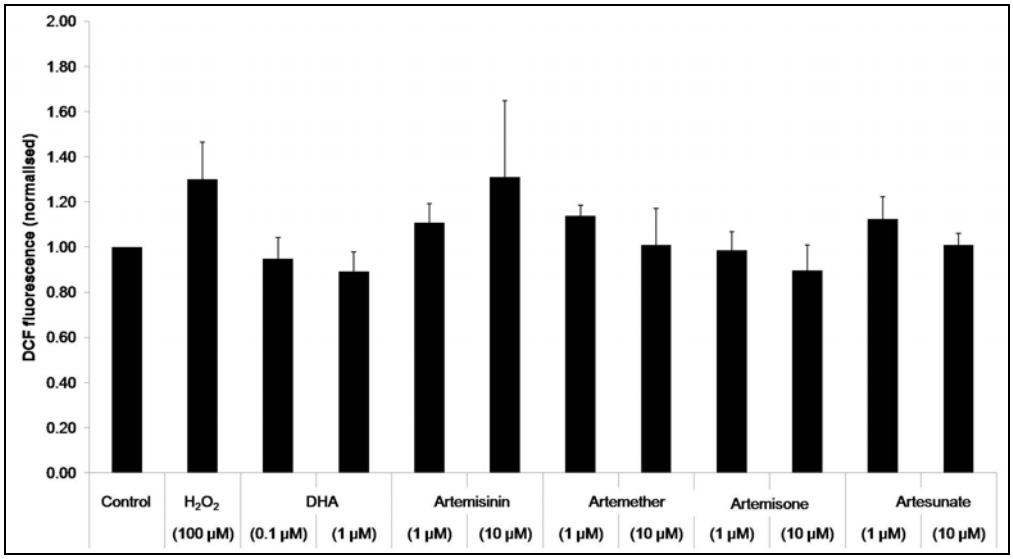


**Figure 12:** DCF fluorescent signals obtained with drug treatment of trophozoite stage parasites. Data are normalized to untreated controls. Values are depicted as mean ± SD from one experiment done in triplicate.

## 4. Discussion

When using the SYBR green efficacy assay and the *P. falciparum* 3D7 strain, the Pheroid® drug delivery system improved the efficacy of artemisone against the parasites. This does not agree with the results obtained with various other *P. falciparum* strains evaluated in Chapter 4. Exactly the same Pheroid® formulation was used for both assays but the method of detection was different. In this study, the SYBR green assay was used, whereas the isotopic $^{3}$H-hypoxanthine growth inhibition assay was used in Chapter 4. Although the $IC_{50}$ values of the two artemisone test formulations (0.001% and 0.002%) were not statistically different, the lower concentration Pheroid® had a lower $IC_{50,}$ which is also strange. The Pheroid® concentration used in Chapter 4 was 0.002%. The $IC_{50}$ values (3.35 ± 0.82 nM) for artemisone is approximately three fold higher than the $IC_{50}$ values (0.88 ± 0.59) reported in the literature (Vivas *et al.,* 2007) with the *P. falciparum* 3D7 strain when using the isotopic $^{3}$H-hypoxanthine growth inhibition assay. Therefore, we contemplate that the SYBR green assay might not be the best assay to evaluate the *in vitro* efficacy of artemisone.

Antibody-mediated growth inhibition of blood stage *P. falciparum* occurred when combined with Vervet monkey plasma. This may indicate that these monkeys are protected against malaria infection. *Aotus* monkeys are one of the few nonhuman primates that are susceptible to infection with the human malaria parasite (Singh *et al.,* 2006).

The antibodies may protect against parasitaemia by means of one or more of the following mechanisms:

i) antibodies directed against proteins expressed by merozoites and subsequent intraerythrocytic developmental stages of the parasite might inhibit erythrocyte invasion and growth (Marsh & Kinyanjui, 2006);
ii) antibodies to a limited set of antigens might inhibit intraerythrocytic parasite growth by means of antibody-dependent mononuclear cell cytokine-mediated inhibition (Bouharoun-Tayoun *et al*., 1990; Bouharoun-Tayoun *et al*., 1995); or
iii) antibodies to parasite antigens expressed on the erythrocyte surface might mediate sequestration and phagocytosis of malaria-infected erythrocytes in the spleen (Berendt *et al*., 1994; Bull *et al*., 2002; Newbold *et al*., 1997).

Monkey plasma, either drug free, or containing artemisone was heat inactivated or treated with protein A gel to remove any growth-inhibitory activity encountered in plasma. This proved useful in the elimination of the growth-inhibitory activity of drug free plasma. The plasma samples collected from healthy monkey subjects during the PK study could not be analysed by the bioassay since the method did not prove to be sensitive or reproducible for

the detection of the antimalarial activities of artemisone in monkey plasma. This study should be repeated using a different method for antimalarial drug susceptibility testing, such as the $^{3}$H-hypoxanthine isotope or the non-isotopic HRP2 ELISA method, since the plasma may have had an influence on the fluorescence produced in the SYBR green assay.

As for the ROS assay, dual labelling with SYTO 61 and CM-$H_2$DCFDA proved useful to distinguish between uninfected and *P. falciparum* infected red blood cells. The DCF signal increased as the parasite progressed to the trophozoite stage, which is consistent with increased metabolic activity and ROS production.

The positive control, $H_2O_2$, as well as the various artemisinin drugs did, however, not increase ROS production in the malaria parasite. Red blood cells contain excessive levels of catalase, which is able to decompose hydrogen peroxide to water and oxygen (Eaton *et al.*, 1972). In a study of Fu *et al.* (2010), RBCs were treated with hydrogen peroxide and only a slight increase in DCF fluorescence as compared to control RBCs was observed with the highest concentration tested (1 mM). When the catalyse activity was inhibited, the DCF signal increased to 15-fold with hydrogen peroxide (Fu *et al.*, 2010). ROS are all highly reactive toward cellular antioxidants and unless intracellular concentrations of $DCFH_2$ are greater than several millimolar, it cannot compete effectively with the endogenous antioxidants for reaction with the ROS (Wrona *et al.*, 2005). Therefore, the $DCFH_2$ probe response may be under non-saturating conditions and will vary with fluctuations in probe loading and/or antioxidant concentrations.

Dichlorodihydrofluorescein ($DCFH_2$) is by far the most widely used probe. However, $DCFH_2$ has very low reactivity toward the two common “reactive oxygen species” in biology namely superoxide ion ($O_2^{\bullet -}$) and hydrogen peroxide ($H_2O_2$) (Wardman, 2007).

Several other limitations for the $DCFH_2$-DA probe exist:

1. DCF fluorescence cannot be used as a direct measure of $H_2O_2$ since $DCFH_2$ does not directly react with $H_2O_2$ to form the fluorescent product, DCF (Kalyanaraman *et al.*, 2012).
2. $DCFH_2$ will also be oxidized to DCF by one-electron-oxidizing species such as hydroxyl radical, species that form peroxidase or the reaction of ferrous iron or ferrous heme with $H_2O_2$. It also reacts with nitrogen dioxide ($NO_2$) formed from the myeloperoxidase/$H_2O_2$/$NO_2^-$ system, hypochlorous acid (HOCl), and various ROS formed from peroxynitrite (ONOO–/ONOOH) decomposition (Kalyanaraman *et al.*, 2012).

3. The intermediate radical ($DCF^{\bullet-}$) formed from the one-electron oxidation of $DCFH_2$ rapidly reacts with $O_2$ to form superoxide ($O_2^{\bullet-}$), which in turn yields additional $H_2O_2$ (Folkes *et al*., 2009). The $H_2O_2$ can engage in redox-cycling with ferrous iron that generates hydroxyl radicals according to the above; overall this will result in the amplification of the fluorescence signal.
4. During apoptosis, cytochromec, a heme protein, is released from mitochondria to the cytosol and that also has the ability to oxidize $DCFH_2$ to DCF (Karlsson *et al*., 2010; Burkitt & Wardman, 2001).
5. Redox-active metals such as $Fe^{2+}$act as catalysts via Fenton chemistry to promote the oxidation of $DCFH_2$ in the presence of oxygen or $H_2O_2$ (Qian & Buettner, 1999). Ferric iron should also be capable of oxidizing $DCFH_2$ especially when ionized in the intracellular medium at pH ~7.3 in accordance with the well-known ability of ferric iron to oxidize phenols to free radicals.
6. The formation of DCF is also pH sensitive. Therefore, if the pH changes inside the RBC or parasite, which can take place with several drugs, the quantity of DCF formed may be different (Mordon *et al*., 1994).
7. An inherent problem of the $H_2$DCFDA probe is the uneven uptake in tissues. This makes it difficult to discriminate an uneven indicator distribution from an uneven ROS distribution (Kristiansen *et al*., 2009).

The current study was based upon that of Klonis *et al.* (2011). The artemisinin-induced increase in oxidative stress was inhibited by hemoglobinase inhibitors and, therefore, the authors concluded that hemoglobin digestion is a requirement for the downstream effect of artemisinin. Hemoglobinase inhibitors inhibit Falcipain-2, a cysteine protease hemoglobinase initiating haemoglobin degradation in the malaria parasite (Chugh *et al*., 2012). Therefore, in the presence of hemoglobinase inhibitors, hemoglobin is not degraded in the malaria parasite's digestive vacuole and heme is not released and polymerized into hemozoin (Sherman, 1979; Fitch *et al.,* 1982). This is proven by a study where treatment with hemoglobinase inhibitors resulted in an accumulation of hemoglobin in the digestive vacuole of the malaria parasite (Rosenthal, 2004). Since heme is not produced, it cannot catalyze the $DCFH_2$ probe reaction with ROS. In addition, haemoglobin degradation in the parasite food vacuole results in the formation of superoxide anion radicals ($O_2^{\bullet-}$), which is rapidly converted to hydrogen peroxide ($H_2O_2$) (Becker *et al*., 2004). If this is reaction is inhibited, the DCF signal will decrease. Thus, the conclusion of Klonis *et al*, (2011) cannot be verified as the current study showed that artemisinins had no effect on ROS production in the malaria parasite.

## 5. Conclusion

Antibody-mediated growth inhibition of blood stage *P. falciparum* occurred with Vervet monkey plasma. After heat inactivation or protein A gel treatment, the Vervet monkey plasma samples from the PK study could not be analysed by the bioassay.

Dual labelling with SYTO 61 and CM-$H_2$DCFDA proved useful to distinguish between uninfected and *P. falciparum* infected red blood cells by means of flow cytometry but this method could not be used to detect ROS formed when infected red blood cells were treated with artemisinin drugs.

## 6. References


Becker, K., Tilley, L., Vennerstrom, J.L., Roberts, D., Rogerson, S. & Ginsburg, H. 2004. Oxidative stress in malaria parasite-infected erythrocytes: Host–parasite interactions. *International journal for parasitology,* 34(2):163.

Bennett, T.N., Paguio, M., Gligorijevic, B., Seudieu, C., Kosar, A.D., Davidson, E. &Roepe, P.D. 2004. Novel, rapid, and inexpensive cell-based quantification of antimalarial drug efficacy. *Antimicrobial agents and chemotherapy,* 48(5):1807-1810.

Berendt, A.R., Ferguson, D.J., Gardner, J., Turner, G., Rowe, A., McCormick, C., Roberts, D., Craig, A., Pinches, R. & Elford, B.C. 1994. Molecular mechanisms of sequestration in malaria. *Parasitology,* 108.

Bonini, M.G., Rota, C., Tomasi, A. & Mason, R.P. 2006. The oxidation of 2',7'-dichlorofluorescin to reactive oxygen species: A self-fulfilling prophesy? *Free radical biology & medicine,* 40(6):968-975.

Bouharoun-Tayoun, H., Attanath, P., Sabchareon, A., Chongsuphajaisiddhi, T. &Druilhe, P. 1990. Antibodies that protect humans against plasmodium falciparum blood stages do not on their own inhibit parasite growth and invasion in vitro, but act in cooperation with monocytes. *Journal of experimental medicine,* 172(6):1633-1641.

Bouharoun-Tayoun, H., Oeuvray, C., Lunel, F. &Druilhe, P. 1995. Mechanisms underlying the monocyte-mediated antibody-dependent killing of plasmodium falciparum asexual blood stages. *Journal of experimental medicine,* 182(2):409-418.

Bull, P.C., Lowe, B.S., Kaleli, N., Njuga, F., Kortok, M., Ross, A., Ndungu, F., Snow, R.W. & Marsh, K. 2002. Plasmodium falciparum infections are associated with agglutinating antibodies to parasite-infected erythrocyte surface antigens among healthy kenyan children. *The journal of infectious diseases,* 185(11):1688-1691.

Burkitt, M.J. &Wardman, P. 2001. Cytochrome c is a potent catalyst of dichlorofluorescin oxidation: Implications for the role of reactive oxygen species in apoptosis. *Biochemical and biophysical research communications,* 282(1):329-333.

Cathcart, R., Schwiers, E. & Ames, B.N. 1984. Detection of picomole levels of lipid hydroperoxides using a dichlorofluorescein fluorescent assay. *Methods in enzymology,* 105352-358.

Chugh, M., Sundararaman, V., Kumar, S., Reddy, V.S., Siddiqui, W.A., Stuart, K.D. & Malhotra, P. 2013. Protein complex directs hemoglobin-to-hemozoin formation in plasmodium falciparum. *Proceedings of the national academy of sciences of the united states of america,* 110(14):5392-5397.

COHEN, G. & HOCHSTEIN, P. 1963. Glutathione peroxidase: The primary agent for the elimination of hydrogen peroxide in erythrocytes. *Biochemistry,* 21420-1428.

Eaton, J.W., Boraas, M. &Etkin, N.L. 1972. Catalase activity and red cell metabolism. *Advances in experimental medicine and biology,* 28121-131.

F, G.G., N, K.H., R, M. & M, F.A. 1994. Importance of catalase in the disposal of hydrogen peroxide within human erythrocytes. *Blood,* 84(1):325-30.

Fishwick, J., McLean, W.G., Edwards, G. & Ward, S.A. 1995. The toxicity of artemisinin and related compounds on neuronal and glial cells in culture. *Chemico-biological interactions,* 96(3):263-271.

Fitch, C.D., Chevli, R., Banyal, H.S., Phillips, G., Pfaller, M.A. &Krogstad, D.J. 1982. Lysis of plasmodium falciparum by ferriprotoporphyrin IX and a chloroquine-ferriprotoporphyrin IX complex. *Antimicrobial agents and chemotherapy,* 21(5):819-822.

Folkes, L.K., Patel, K.B., Wardman, P. &Wrona, M. 2009. Kinetics of reaction of nitrogen dioxide with dihydrorhodamine and the reaction of the dihydrorhodamine radical with oxygen: Implications for quantifying peroxynitrite formation in cells. *Archives of biochemistry & biophysics,* 484(2):122-126.

Gabriel, J. &Berzins, K. 1983. Specific lysis of plasmodium yoelii infected mouse erythrocytes with antibody and complement. *Clinical & experimental immunology,* 52(1):129-134.

Goldberg, D.E., Slater, A.F.G., Beavis, R., Chait, B., Cerami, A. & Henderson, G.B. 1991. Hemoglobin degradation in the human malaria pathogen plasmodium falciparum: A catabolic pathway initiated by a specific aspartic protease. *Journal of experimental medicine,* 173(4):961-969.

Haynes, R.K., Fugmann, B., Stetter, J., Rieckmann, K., Heilmann, H., Chan, H., Cheung, M., Lam, W., Wong, H., Croft, S.L., Vivas, L., Rattray, L., Stewart, L., Peters, W., Robinson, B.L., Edstein, M.D., Kotecka, B., Kyle, D.E., Beckermann, B., Gerisch, M., Radtke, M., Schmuck, G., Steinke, W., Wollborn, U., Schmeer, K. &Römer, A. 2006. Artemisone--a highly active antimalarial drug of the artemisinin class. *Angewandte chemie (international ed.in english),* 45(13):2082-2088.

Hempel, S.L., Buettner, G.R., O'Malley, ,Y.Q., Wessels, D.A. & Flaherty, D.M. 1999. Dihydrofluorescein diacetate is superior for detecting intracellular oxidants: Comparison with 2',7'-dichlorodihydrofluorescein diacetate, 5(and 6)-carboxy-2',7'-dichlorodihydrofluorescein diacetate, and dihydrorhodamine 123. *Free radical biology & medicine,* 27(1-2):146-159.

Jokerst, J.V., Lobovkina, T., Zare, R.N. &Gambhir, S.S. 2011. Nanoparticle PEGylation for imaging and therapy. *Nanomedicine (london, england),* 6(4):715-728.

Jourdan, J. 2011. Evaluation of the pheroid™ technology to improve the *in vitro* activity of antimalarial drugs. , Switzerland: Swiss Tropical and Public Health Institute (Dissertation – MSc).

Kalyanaraman, B., Darley-Usmar, V., Davies, K.J.A., Dennery, P.A., Forman, H.J., Grisham, M.B., Mann, G.E., Moore, K., Roberts, L.J. &Ischiropoulos, H. 2012. Measuring reactive oxygen and nitrogen species with fluorescent probes: Challenges and limitations. *Free radical biology & medicine,* 52(1):1-6.

Klonis, N., Crespo-Ortiz, M., Bottova, I., Abu-Bakar, N., Kenny, S., Rosenthal, P.J. & Tilley, L. 2011. Artemisinin activity against plasmodium falciparum requires hemoglobin uptake and digestion. *Proceedings of the national academy of sciences of the united states of america,* 108(28):11405-11410.

Kotecka, B.M. &Rieckmann, K.H. 1993. Chloroquine bioassay using malaria microcultures. *American journal of tropical medicine and hygiene,* 49(4):460-464.

Kristiansen, K.A., Jensen, P.E., Møller, I.M. & Schulz, A. 2009. Monitoring reactive oxygen species formation and localisation in living cells by use of the fluorescent probe CM-H2DCFDA and confocal laser microscopy. *Physiologiaplantarum,* 136(4):369-383.

Krungkrai, S.R. &Yuthavong, Y. 1987. The antimalarial action on plasmodium falciparum of qinghaosu and artesunate in combination with agents which modulate oxidant stress. *Transactions of the royal society of tropical medicine and hygiene,* 81(5):710-714.

Lambros, C. &Vanderberg, J.P. 1979. Synchronization of plasmodium falciparum erythrocytic stages in culture. *The journal of parasitology,* 65(3):418-420.

LeBel, C.P., Ischiropoulos, H. &Bondy, S.C. 1992. Evaluation of the probe 2',7'-dichlorofluorescin as an indicator of reactive oxygen species formation and oxidative stress. *Chemical research in toxicology,* 5(2):227-231.

LeBel, C.P., Ischiropoulos, H. &Bondy, S.C. 1992. Evaluation of the probe 2',7'-dichlorofluorescin as an indicator of reactive oxygen species formation and oxidative stress. *Chemical research in toxicology,* 5(2):227-231.

Levander, O.A., Ager, A.L., J., Morris, V.C. & May, R.G. 1989. Qinghaosu, dietary vitamin E, selenium, and cod-liver oil: Effect on the susceptibility of mice to the malarial parasite plasmodium yoelii. *The american journal of clinical nutrition,* 50(2):346-352.

Maldiney, T., Richard, C., Seguin, J., Wattier, N., Bessodes, M. &Scherman, D. 2011. Effect of core diameter, surface coating, and PEG chain length on the biodistribution of persistent luminescence nanoparticles in mice. *ACS nano,* 5(2):854-862.

Markus Karlsson, TinoKurz, Ulf T. Brunk, Sven E. Nilsson & Christina I. Frennesson. 2010. What does the commonly used DCF test for oxidative stress really show? *Biochemical journal,* 428(2):183-190.

MARSH, K. & KINYANJUI, S. 2006. Immune effector mechanisms in malaria. *Parasite immunology,* 28(1):51-60.

McLean, W.G. & Ward, S.A. 1998. In vitro neurotoxicity of artemisinin derivatives. *Médecinetropicale: Revue du corps de santé colonial,* 58(3):28-31.

Meshnick, S.R., Tsang, T.W., Lin, F.B., Pan, H.Z., Chang, C.N., Kuypers, F., Chiu, D. &Lubin, B. 1989. Activated oxygen mediates the antimalarial activity of qinghaosu. *Malaria and the red cell: 2.proceedings of the second workshop on malaria and the red cell, held in annarbor, michigan, USA, october 24, 1988.,* .

Mordon, S., Devoisselle, J.M. &Maunoury, V. 1994. In vivo pH measurement and imaging of tumor tissue using a pH-sensitive fluorescent probe (5,6-carboxyfluorescein): Instrumental and experimental studies. *Photochemistry and photobiology,* 60(3):274-279.

Nagelschmitz, J., Voith, B., Wensing, G., Roemer, A., Fugmann, B., Haynes, R.K., Kotecka, B.M., Rieckmann, K.H. & Edstein, M.D. 2008. First assessment in humans of the safety, tolerability, pharmacokinetics, and ex vivo pharmacodynamic antimalarial activity of the new artemisinin derivative artemisone. *Antimicrobial agents and chemotherapy,* 52(9):3085-3091.

Newbold, C.I., Craig, A.G., Kyes, S., Berendt, A.R., Snow, R.W., Peshu, N. & Marsh, K. 1997. PfEMP1, polymorphism and pathogenesis. *Annals of tropical medicine and parasitology,* 91(5):551-557.

Qian, S.Y. &Buettner, G.R. 1999. Iron and dioxygen chemistry is an important route to initiation of biological free radical oxidations: An electron paramagnetic resonance spin trapping study. *Free radical biology & medicine,* 26(11-12):1447-1456.

Rosenthal, P.J. 2004. Cysteine proteases of malaria parasites. *International journal for parasitology,* 34(13):1489-1499.

Sadzuka, Y., Nakade, A., Hirama, R., Miyagishima, A., Nozawa, Y., Hirota, S. &Sonobe, T. 2002. Effects of mixed polyethyleneglycol modification on fixed aqueous layer thickness and antitumor activity of doxorubicin containing liposome. *International journal of pharmaceutics,* 238(1-2):171-180.

Schmuck, G., Roehrdanz, E., Haynes, R.K. & Kahl, R. 2002. Neurotoxic mode of action of artemisinin. *Antimicrobial agents and chemotherapy,* 46(3):821-827.

Scott, M.D., Meshnick, S.R., Williams, R.A., Chiu, D.T., Pan, H.C., Lubin, B.H. &Kuypers, F.A. 1989. Qinghaosu-mediated oxidation in normal and abnormal erythrocytes. *The journal of laboratory and clinical medicine,* 114(4):401-406.

Sherman, I.W. 1979. Biochemistry of plasmodium [malarial parasites]. *Microbiological reviews*.

Singh, S., Miura, K., Zhou, H., Muratova, O., Keegan, B., Miles, A., Martin, L.B., Saul, A.J., Miller, L.H. & Long, C.A. 2006. Immunity to recombinant plasmodium falciparum merozoite surface protein 1 (MSP1): Protection in aotusnancymai monkeys strongly correlates with anti-MSP1 antibody titer and in vitro parasite-inhibitory activity. *Infection and immunity,* 74(8):4573-4580.

Smilkstein, M., Sriwilaijaroen, N., Kelly, J.X., Wilairat, P. &Riscoe, M. 2004. Simple and inexpensive fluorescence-based technique for high-throughput antimalarial drug screening. *Antimicrobial agents and chemotherapy,* 48(5):1803-1806.

Steyn, J.D. 2009. Novel artemisinin derivatives with pheroid™ technology for malaria treatment. Potchefstroom: NWU. (Thesis – PhD).

Teja-Isavadharm, P., Peggins, J.O., Brewer, T.G., White, N.J., Webster, H.K. & Kyle, D.E. 2004. Plasmodium falciparum-based bioassay for measurement of artemisinin derivatives in plasma or serum. *Antimicrobial agents and chemotherapy,* 48(3):954-960.

Vivas, L., Rattray, L., Stewart, L.B., Robinson, B.L., Fugmann, B., Haynes, R.K., Peters, W. & Croft, S.L. 2007. Antimalarial efficacy and drug interactions of the novel semi-synthetic endoperoxide artemisone in vitro and in vivo. *Journal of antimicrobial chemotherapy (JAC),* 59(4):658-658.

Wang, J., Huang, L., Li, J., Fan, Q., Long, Y., Li, Y. & Zhou, B. 2010. Artemisinin directly targets malarial mitochondria through its specific mitochondrial activation. *Plos one,* 5(3):1-12.

Wardman, P. 2007. Fluorescent and luminescent probes for measurement of oxidative and nitrosative species in cells and tissues: Progress, pitfalls, and prospects. *Free radical biology & medicine,* 43(7):995-1022.

Wesche, D.L., DeCoster, M.A., Tortella, F.C. & Brewer, T.G. 1994. Neurotoxicity of artemisininanalogs in vitro. *Antimicrobial agents and chemotherapy,* 38(8):1813-1819.

Wissing, F., Sanchez, C.P., Rohrbach, P., Ricken, S. &Lanzer, M. 2002. Illumination of the malaria parasite plasmodium falciparum alters intracellular pH: Implications for live cell imaging. *Journal of biological chemistry,* 277(40):37747-37755.

Wrona, M., Patel, K. &Wardman, P. 2005. Reactivity of 2',7'-dichlorodihydrofluorescein and dihydrorhodamine 123 and their oxidized forms toward carbonate, nitrogen dioxide, and hydroxyl radicals. *Free radical biology & medicine,* 38(2):262-270.

Zielonka, J. &Kalyanaraman, B. 2008. "ROS-generating mitochondrial DNA mutations can regulate tumor cell metastasis"--a critical commentary. *Free radical biology & medicine,* 45(9):1217-1219.